# DEVELOPMENT OF THE UNIVERSITY COLLEGE DUBLIN HOLLOW CYLINDER APPARATUS

Brendan C. O'Kelly, Trinity College, Dublin, Ireland. Formerly Scott Wilson, UK
Patrick J. Naughton, National University of Ireland, Galway, Ireland

ABSTRACT: The principal mechanical components, instrumentation and operation of a new hollow cylinder apparatus for generalised stress path testing of soil are presented. Using the apparatus, axial and torsional loads are applied to the ends of the hollow cylindrical specimen that is subjected to lateral confining pressures inside a pressure cell. The automated apparatus is capable of regulating the induced sample stresses to 0.5kPa during testing. Accurate measurement of the mechanical and pore pressure responses of the test specimen from the pseudo-elastic domain to sample failure is facilitated. Control programs continually regulate the induced stresses, based on the updated sample geometry, to accurately follow the prescribed stress paths. Proving test results are presented to demonstrate the capability of the new apparatus to accurately follow complex stress paths.

RÉSUMÉ: Les composants mécaniques principaux, l'instrumentation et le principe du nouvel appareil à cylindre creux, utilisé pour tester la trajectoire d'une contrainte généralisée d'un sol, sont presentés. Avec cet appareil, des charges axiales et de torsion sont appliquées aux extremités du cylindre creux, lui-meme exposé à des pressions latérales de confinement a l'intérieur d'une cellule pressurisée. L'appareil automatisé est capable de réguler des pressions échantillons exercées à 0.5 kPa au cours de ces tests. Des mesures précises des réponses mécaniques et de pores de pression de l'appareil testé sont effectuées afin d'évaluer les défauts (echecs) dans le domaine pseudo-elastic. Des programmes de controle permettent de réguler les stress appliqués, basés sur des exemples récents de géométrie, afin de suivre précisement les trajectoires de contraintes voulues. Des résultats d'essais probants sont présentés afin de prouver les capacités du nouvel appareil pour le suivi précis de trajectoires complexes de contraintes.

## 1. INTRODUCTION

Fundamental to soil mechanics design is the accurate determination of the mechanical and pore-pressure responses of the ground to applied loads. However, laboratory-measured strength and stiffness values are often inconsistent with the values that are obtained from back-analysis of the ground performance, principally due to limitations of standard test apparatus (which facilitate limited sample loading and boundary conditions) and sample disturbance effects. For example, the Bishop & Wesley stress path and triaxial apparatus can only subject the test specimen to axi-symmetric loading conditions. Most ground engineering problems, however, involve multi-directional loading that invariably causes reorientation of the principal stress axes and changes in the relative magnitude of the intermediate principal stress in the ground. The more sophisticated hollow cylinder apparatus (HCA) allows independent control of the magnitude of the three principal stresses and rotation of the major-minor principal stress axes facilitating more generalised stress path testing. Although such apparatus are still rare, their development and use has steadily increased, principally at leading research establishments, (Hight *et al*. 1983; Vaid *et al*. 1990; Ampadu and Tatsuoka, 1993).

A new automated HCA has recently been developed (O'Kelly, 2000) and automated (Naughton, 2003) at the Department of Civil Engineering, University College Dublin (UCD), Ireland. The new apparatus facilitates generalised stress path testing with accurate measurement of the mechanical and pore-pressure responses of the test specimen from very small strains (of the order of $10^{-5}$ strain) to sample failure. The following sections present the principle of hollow cylinder testing; the research, development and automation of the new apparatus; and the results of some proving tests that demonstrate the apparatus capabilities.

## 2. PRINCIPLE OF HOLLOW CYLINDER TESTING

The sample geometry employed is that of a thick-walled hollow cylinder (Figure 1). Sample dimensions of 100mm outer diameter, 71mm inner diameter and 200mm long were selected. Hydrostatic confining pressures, $p_o$ and $p_i$, are applied to the outer and inner sample walls, respectively (Figure 1(a)). Coaxial (M) and torsional (T) loads are applied to the sample ends via annular platens. Figure 1(b) shows the sample deformational response: v is the axial deformation; $w_o$ and $w_i$ are the radial displacements of the outer and inner walls, respectively; and $\theta$ the sample twist.

Four non-zero polar stresses ($\sigma_z$, $\sigma_r$, $\sigma_\theta$, $\tau_{z\theta}$) are induced in an element of the sample wall (Figure 1(c)). The magnitudes of these stresses are calculated from the applied loads, confining pressures and the deformational response of the sample. The radial confining stress ($\sigma_r$) is

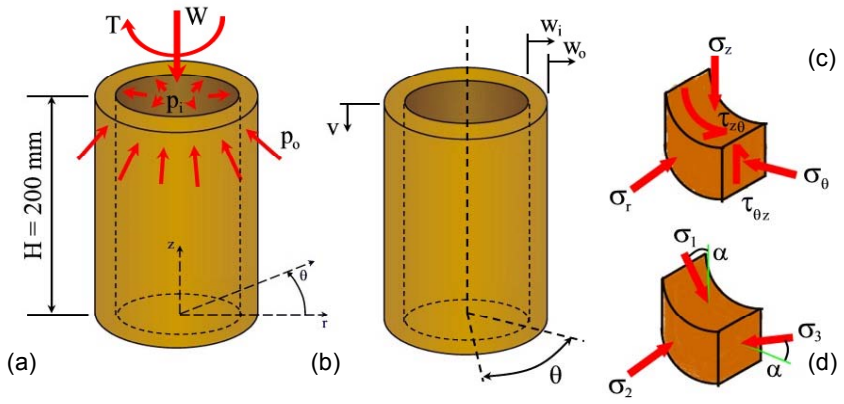


(a) Applied loads, confining pressures; (b) sample deformations; (c) mean stresses; (d) resolved principal stresses.
Figure 1. Stress and deformation states of the hollow cylindrical sample.

a principal stress, usually the intermediate principal stress ($\sigma_2$). Hence, application of the torque causes rotation ($\alpha$) of the major ($\sigma_1$) and minor ($\sigma_3$) principal stress axes in the vertical plane (Figure 1(d)). The magnitude and direction of the major and minor principal stresses are resolved from the four induced polar stresses using the Mohr circle of stress analysis.

Stress (and hence strain) non-uniformity develops across the sample wall whenever a torque and/or unequal confining pressures are applied due to the wall curvature (Wijewickreme and Vaid, 1991). An analysis of possible sample geometries indicated that the selected sample size would result in reasonably homogeneous stress distributions acting across the sample wall for generalised stress conditions.

## 3. THE NEW HOLLOW CYLINDER APPARATUS

### 3.1 Cell loading mechanisms and pressure systems

Figure 2 shows the general arrangement of the new HCA. The traditional HCA layout was rearranged so that the new apparatus is more compact and the pressure cell is more easily assembled and dismantled. The ends of the hollow cylindrical test-specimen are in contact with two annular platens inside the acrylic pressure-cell, 340mm diameter by 600mm high. The test specimen is enclosed between outer and inner rubber membranes. The outer cell chamber and the inner bore cavity of the sample are independently sealed. Figure 3 shows the specimen and inner bore cavity seals at the loading platen. Digital pressure-volume controllers (from GDS Instruments Ltd.) independently control the hydraulic confining pressures (applied to the cell chamber and bore cavity) and the sample back-pressure (applied to the base of the test-specimen). The acrylic pressure cylinder limits the rated working pressure to 1.0MPa. The cell tie bars, connecting the cell top and base plates, are located inside the acrylic cylinder. All load-bearing components inside the cell were manufactured from grade 316, stainless steel. Pneumatic mounts separating the pressure cell from the steel support frame isolate the cell (and hence the test specimen) from external vibrations to facilitate reliable small-strain sample measurements. Special instrument housings were also developed to waterproof instrumentation submerged inside the pressure-cell.

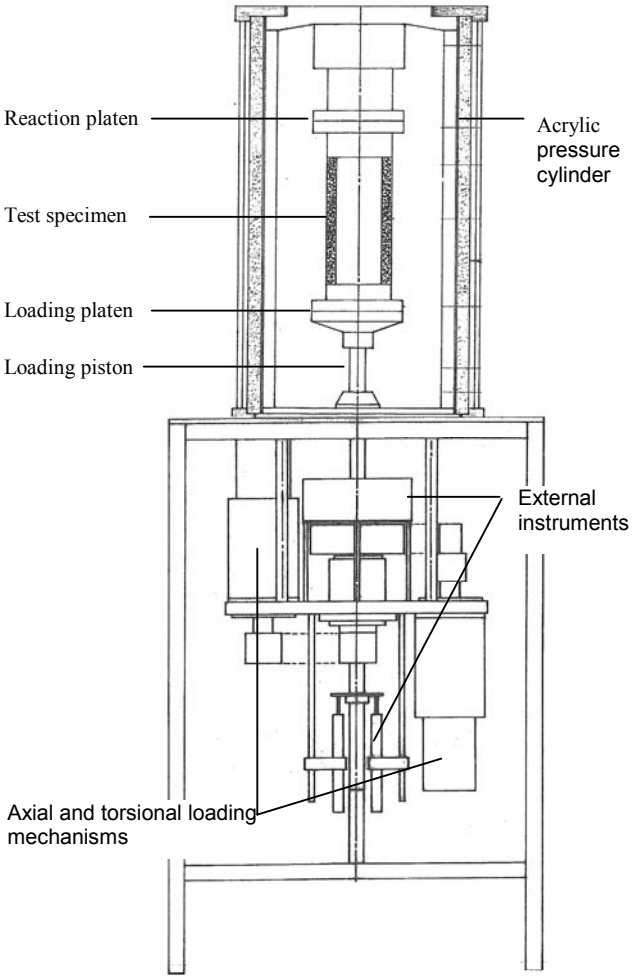


Figure 2. Schematic of UCD hollow cylinder apparatus.

Axial and twist boundary displacements are applied via the 25mm diameter loading piston to the base of the sample which is restrained at its upper end. Eight thin, radial blades protruding above the rough annular porous discs, which are fastened to the loading and reaction platens, ensure full torque transmission.

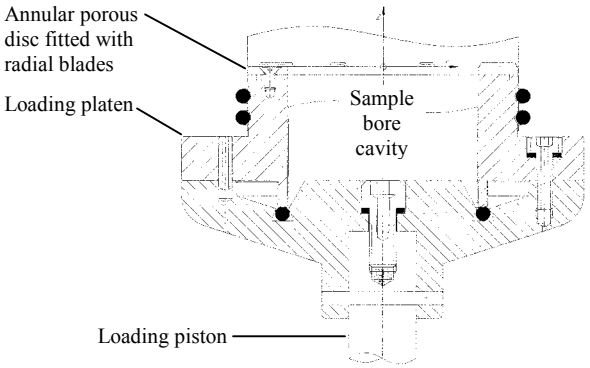


Figure 3: The loading platen assembly.

Innovative mechanisms to displace and rotate the loading piston, which passes through the cell base, are secured to the reaction frame located beneath the cell. Screw and spline type ball bearings, integrated about the lower end of the piston, facilitate smooth vertical, rotary and spiral piston motions. Drive units, which consist of a motor and precision gearbox, are coupled to the screw and spline bearings using pre-tensioned block and tackle linkages. The rated axial and torsional working loads of the mechanisms are 19.3kN and $\pm$103N.m, respectively (corresponding to unconfined compressive and torsional shear stresses of 5.0MPa and $\pm$0.6MPa, respectively). The equivalent dynamic load values are 9.1kN and $\pm$105N.m, respectively. The working stress domain facilitates generalised stress path testing, to failure, of all geomaterials (including soft to weak rock) at the maximum confining cell pressure of 1.0MPa. Axial and rotary slack (when the loading directions are reversed) in the mechanisms is limited to 1$\mu$m and 15 arc-seconds, respectively. The stiffness of the loading mechanisms so achieved facilitates accurate static, cyclic and dynamic testing.

### 3.2 Instrumentation and automation

The new HCA is automatically closed-loop controlled to facilitate generalised stress path testing from the small strain domain (of the order of $10^{-5}$ strain) to sample failure. The three GDS controllers independently measure and control the applied pressures and volume changes of the outer cell and inner bore chambers and the test specimen. A differential pressure transducer measures the effective confining pressure acting on the sample.

Instruments located inside the pressure cell measure the axial and torsional loads (developed across the sample length) and the polar deformational response of the sample. The induced loads are measured using a combined thrust-torque transducer, which is incorporated in the sample reaction platen (Figure 4). Three Imperial College inclinometer gauges (Symes and Burland, 1984), which were modified to the author's design, and two proximity transducers measure sample strains over the mid-third of the sample length to a resolution of better than $5\times10^{-5}$ strain. Deformations are measured locally over the central gauge length of the sample to exclude errors due to apparatus compliance and sample end-restraint and bedding effects. The inclinometer gauges are attached to the outer sample membrane and measure axial and twist deformations of the sample. Proximity transducers located in the outer cell and inner bore chambers measure radial displacements of the sample walls. These non-contact transducers use the principal of impedance variation to measure the gaps between the transducer faces and aluminium foil targets which are attached to the rubber membranes that enclose the sample. These transducers can be remotely deployed and repositioned from outside the pressure-cell during a test.

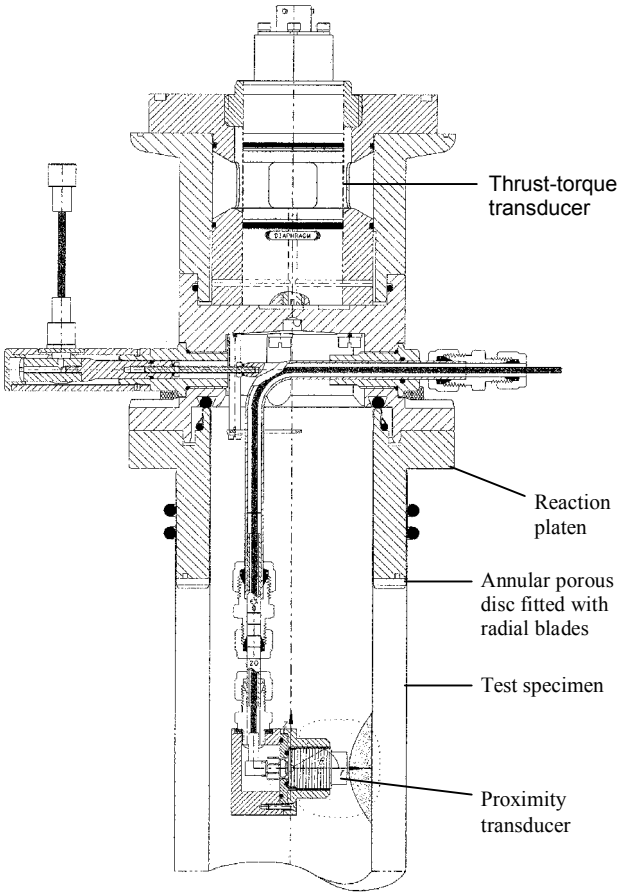


Figure 4. The reaction-platen assembly.

Backup sample deformation measurements are also provided from outside the cell by two displacement transducers and a rotary encoder which measure the axial and rotary piston movements and hence the applied axial and twist sample boundary displacements. Special calibration procedures, which improve the instrument accuracy relative to that achieved by other apparatus,

were developed for several of the instruments. For example, the proximity transducers are calibrated using an optical table and laser measurement system.

Stepper motors drive the mechanisms that apply the axial and twist boundary displacements to the sample ends. A suite of LabVIEW programs were developed to automatically closed-loop control the apparatus to facilitate generalised stress path testing. The control programs interface with the stepper motors, the GDS pressure-volume controllers and the instruments via a data-acquisition system to control the magnitudes of the four induced sample stresses ($\sigma_z$, $\sigma_r$, $\sigma_\theta$, $\tau_{z\theta}$) to within 0.5kPa of the targeted values. Algorithms were developed to enhance the pressure resolution of the standard controllers from GDS Instruments Ltd. The control programs automatically correct for membrane penetration and membrane restraint effects on the sample. Axial and twist sample boundary displacements are applied in 0.1$\mu$m and 0.8 arc-second steps (equivalent to strain resolutions of better than $7x10^{-7}$ strain) by the loading mechanisms. The control programs continuously compute the current stress state and the sample strain response from the load-pressure-deformation instrument readings.

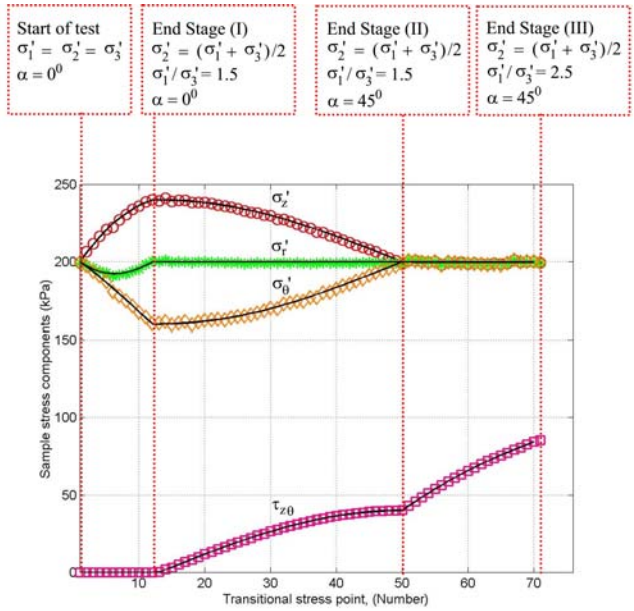


Figure 5. Targeting of transitional stress points to follow a prescribed stress path.

Prescribed generalised stress paths are followed by sequentially moving between transitional target stress points located along the stress paths (Figure 5). The control programs command the stepper motors and controllers to simultaneously adjust the sample stresses to arrive at the next stress point on the stress path, and the process repeated. For example, the solid lines in Figure 5 represent a predefined three sequential stress paths while the data points represent actual transitional stress points achieved by the apparatus. Starting from an isotropic stress state of 200kPa, the test specimen was consolidated vertically creating a cross-anisotropic soil fabric, (stage I). The major-minor principal stress axes were rotated (from the vertical direction) through 45 degrees, (stage II). The principal stress magnitudes were increased while the major principal stress axis remained fixed, (stage III).

## 4. RESULTS OF PROVING TESTS

The test capabilities of the new HCA were investigated by requesting the apparatus to follow both isotropic and anisotropic stress paths. The test material was well-graded, fine-to-medium, white Leighton Buzzard sand (Table 1).

Table 1. Some physical properties of Leighton Buzzard sand tested.

| Property | Coefficient of uniformity | Coefficient of curvature | Particle density, ($Mg/m^3$) | Max void ratio | Min void ratio |
|---|---|---|---|---|---|
| Value | 1.32 | 0.96 | 2.64 | 0.77 | 0.50 |

Three identical medium-to-dense sand specimens were subjected to isotropic stress paths that increased the mean effective stress in the samples from 50kPa to 200kPa. Good repeatability of the principal and volumetric strains was achieved (Figure 6) indicating both the reliability of the sample preparation method and the ability of the apparatus to record consistent stress-strain responses.

Anisotropic stress paths, where the stress state of identical sand test specimens was changed along three different stress paths, are presented (Figure 7). The stress paths involved anisotropic consolidation (quantified in terms of the effective principal stress ratio, R' = $\sigma_1'/\sigma_3'$) and rotation ($\alpha_\sigma$) of the major principal stress direction. The actual mean induced stresses deviated by less than $\pm$ 2.5 % from their target values for these stress paths.

The stress paths followed describe smooth curves when plotted in terms of the shear stress to normal stress difference (Figure 8). The increment stress changes along these stress paths define the rotation of the major principal stress increment direction ($\alpha_{\Delta\sigma}$). Tests A and B follow stress paths where $\alpha_{\Delta\sigma}$ should be identical between Points B and E in Test A and Points C and D in Test B.

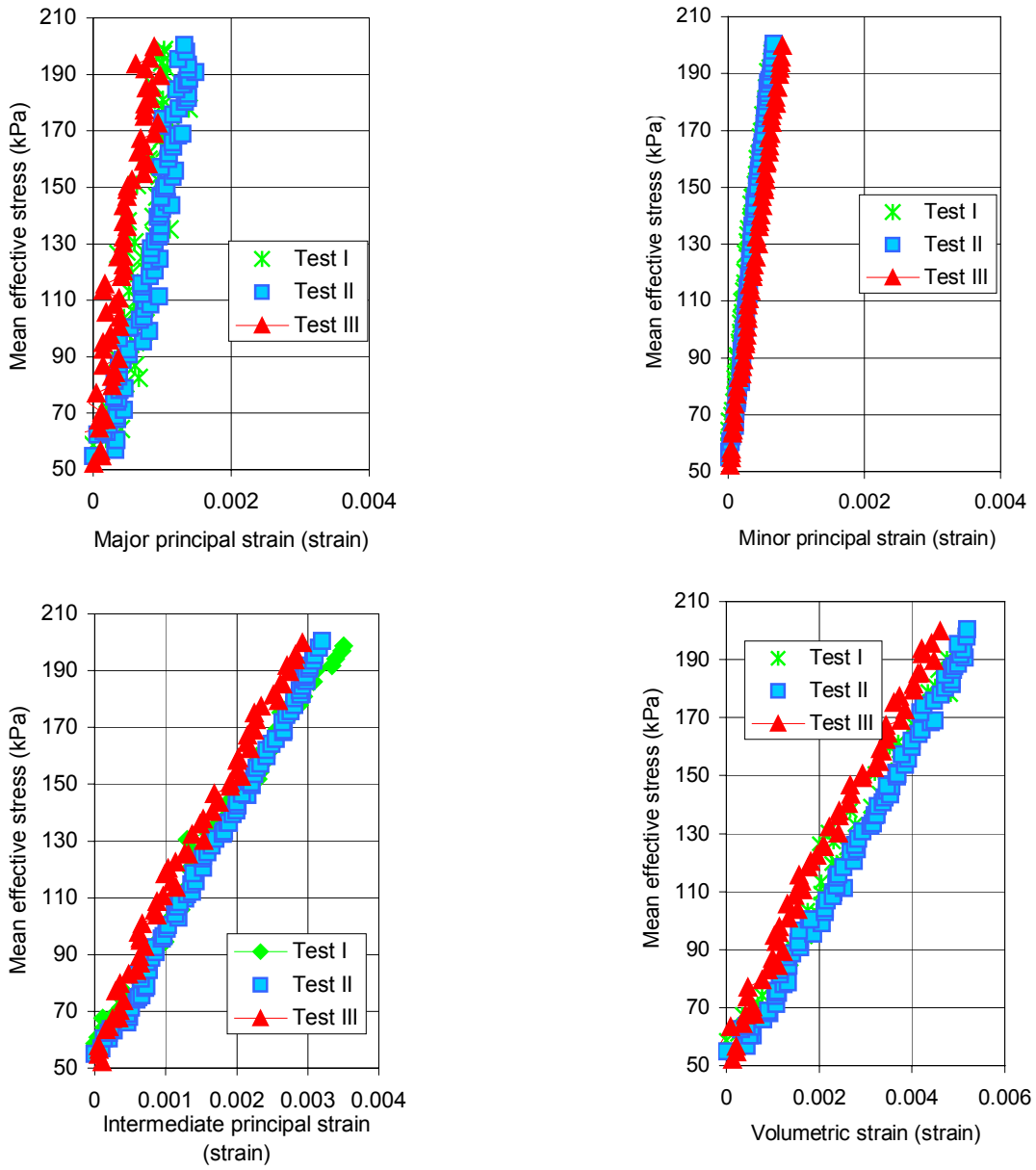


Figure 6. Stress-strain responses of isotropically consolidated test specimens in terms of (a) major (b) intermediate (c) minor principal strains, and (d) volumetric strain.

The principal stress increment directions do not coincide with the existing principal stress directions due to the anisotropy of the soil (Figure 9). However, excellent repeatability of $\alpha_{\Delta\sigma}$ for tests A and B is observed indicating the excellent stress path control achieved by the new apparatus.

## 5. CONCLUDING COMMENTS

The new, state-of-the-art hollow cylinder apparatus, recently developed at University College Dublin, facilitates generalised stress path testing over a wide strain range. Excellent control of the stresses induced in the test specimen can be achieved using the new apparatus. The new apparatus facilitates accurate measurement of the mechanical and pore-pressure responses of soil from the pseudo-elastic soil domain to sample failure. Test data presented in the Paper demonstrate the apparatus capability to consistently measure the stress-strain responses of identical sand specimens and the repeatability of the sample preparation method. The principal stress increment directions were not coincident with the existing principal stress directions due to the anisotropy of the sand test specimens.

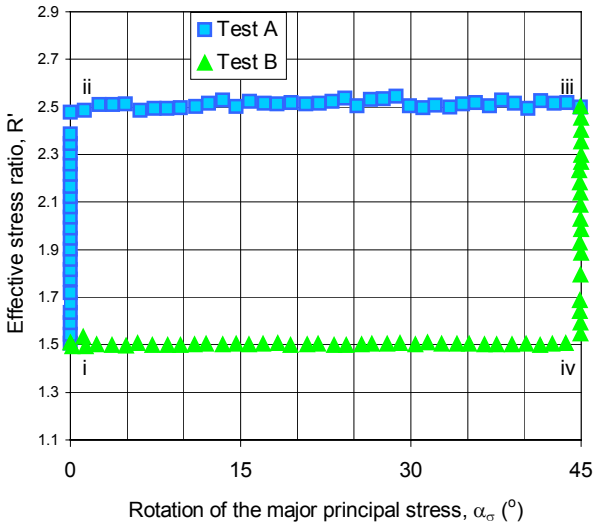


Figure 7. Anisotropic stress paths, expressed in terms of effective stress ratio and major principal stress rotation.

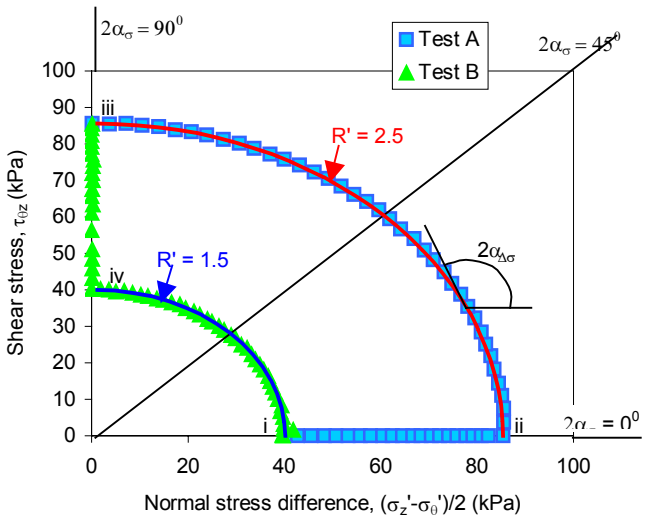


Figure 8. Shear stress to normal stress difference for the proving tests.

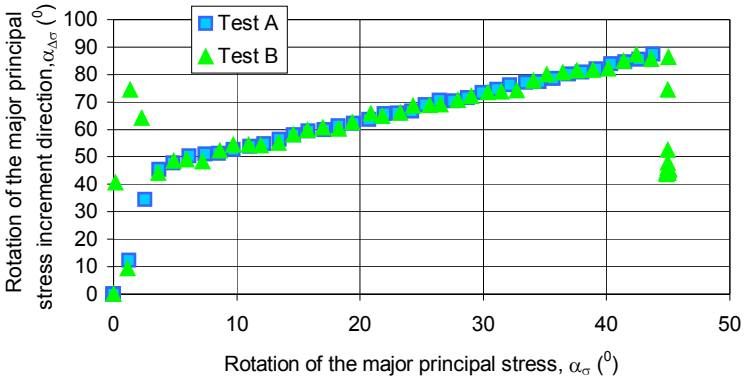


Figure 9. Direction of major principal stress increment relative to direction of major principal stress axis.

## 6. ACKNOWLEDGEMENTS

The authors would like to thank Dr Tom Widdis for his support during the course of this research project. The authors would also like to thank Dr Trevor Orr for his helpful comments during the preparation of this paper.

## 7. REFERENCES

Ampadu, S.K. and Tatsuoka, F. 1993. A hollow cylinder torsional simple shear apparatus capable of a wide range of shear strain measurements. Geotechnical Testing Jornal, 16(1): pp. 14-34.

Hight, D.W., Gens, A. and Symes, M.J. 1983. The development of a new hollow cylinder apparatus for investigating the effects of principal stress rotation in soils. Geotechnique, 33(4): pp. 355-383.

Naughton, P.J. 2002. The investigation of Leighton Buzzard sand in a new hollow cylinder apparatus. Ph.D. Thesis, submitted to University College Dublin, Ireland.

O'Kelly, B.C. 2000. Development of a new apparatus for hollow cylinder testing. Ph.D. Thesis, University College Dublin, Ireland.

Symes, M.J. and Burland, J.B. 1984. Determination of local displacements on soil samples. Geotechnical Testing Journal, 7(2): pp. 49-59.

Vaid, Y.P., Sayao, A., Hou, E. and Negussey, D. 1990. Generalised stress-path-dependent soil behaviour with a new hollow cylinder torsional apparatus. Canadian Geotechnical Journal, 27: pp. 601-616.

Wijewickreme, D. and Vaid, Y.P. 1991. Stress nonuniformities in hollow cylinder torsional specimens. Geotechnical Testing Journal, 14(4): pp. 349-362.